

Surface Treatment of Garnet-Type Solid Electrolyte for Suppressing Dendritic Growth

Tsuyoshi Ohnishi, Isao Sakaguchi, and Kazunori Takada*

Cite This: *ACS Appl. Energy Mater.* 2024, 7, 5321–5325

Read Online

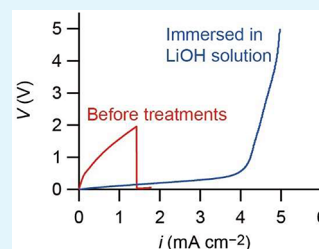
ACCESS |

Metrics & More

Article Recommendations

Supporting Information

ABSTRACT: Garnet-type solid electrolytes are regarded as promising electrolytes for oxide-based solid-state batteries due to their stability against lithium metal. However, lithium metal anodes on garnet-type solid electrolytes often exhibit dendritic growth, leading to internal short-circuit. This study reveals that immersion of the solid electrolytes in an aqueous solution of LiOH is a very simple and effective way to suppress dendritic growth. It removes the contamination layer formed on the electrolyte surface by exposure to ambient air, and it makes the interface to the lithium metal anode conductive and the current density homogeneous.



KEYWORDS: solid electrolyte, garnet, lithium metal, dendrite, critical current density, short-circuit, surface treatment

Garnet-type solid electrolytes are regarded as promising materials for oxide-based solid-state batteries. Among the several kinds of solid electrolytes, e.g., NASICON,¹ perovskite,² and garnet-types,³ having ionic conductivities on the order of 10^{-3} S cm^{-1} at room temperature, garnet-type solid electrolytes exhibit the highest stability against lithium metal anodes,⁴ although recent studies point out that they undergo slight electrochemical reduction in the vicinity of the lithium metal interface.⁵ However, realizing lithium metal anodes in solid-state batteries is still challenging because they often show dendritic growth in garnet-type solid electrolytes, readily leading to internal short-circuit.^{6,7}

The dendritic growth of lithium metal takes place at a high charging current density, which is called the critical current density. The critical current density will strongly depend on the surface chemistry of garnet. For example, exposure of garnet to ambient air forms a contamination layer of Li_2CO_3 and LiOH with protonation of the garnet.^{8,9} Since the contamination layer is a poor ionic conductor, it impedes lithium-ion transfer at the interface to the electrode. Therefore, when a solid-state battery with a lithium metal anode is assembled with such a garnet electrolyte and charged, the charging current is concentrated to part of the Li/garnet interface, where the contamination layer is not formed. In this situation, the solid-state battery is short-circuited easily because the local current density at the interface with the contamination layer is higher than the apparent current density calculated from the projection area of the interface and tends to exceed the critical value for short-circuit. Various methods to remove the contamination layer have been proposed in order to suppress the internal short-circuit: surface polishing,^{10,11} heat treatment to react Li_2CO_3 with protonated garnet,¹² and reacting Li_2CO_3 with carbon.¹³ This paper

provides a very simple method to suppress internal short-circuit effectively.

This study reveals effects of the following treatments on the electrode properties of lithium metal anodes: surface polishing using 400 grit sandpaper, annealing at 700 °C for 2 h under O_2 flow with a flow rate of 200 mL min^{-1} , and immersion in a saturated aqueous solution of LiOH. These treatments are applied to sintered pellets of a garnet-type solid electrolyte one by one in this order. The garnet-type solid electrolyte used in this study is $\text{Li}_{6.6}\text{La}_3\text{Zr}_{1.6}\text{Ta}_{0.4}\text{O}_{12}$. Sintered pellets are 10 mm square and 0.5 mm thick and supplied by Toshiba Manufacturing Co., Ltd. After these treatments, lithium metal electrodes with a thickness of 5 μm are formed on both surfaces of the pellets by thermal evaporation for assembling Li/garnet/Li symmetric cells. Complex impedance of the cells is recorded in the frequency range from 1 MHz to 10 mHz with an ac signal of 20 mV at open-circuit voltage. Effects of the treatments against the internal short-circuit is evaluated by chronopotentiometry with programmed current, in which a ramp-up current of 1 or 5 $\text{mA cm}^{-2} \text{min}^{-1}$ is applied to Li/garnet/Li symmetric cells until the dendritic growth causes short-circuit. No stacking pressure is applied to the cells during the electrochemical measurements.

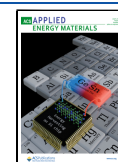
The symmetric cell assembled with the as-supplied sintered pellet without any treatments gives a depressed semicircle in its Nyquist plot, as shown in Figure 1a. Since the diameter of the

Received: April 2, 2024

Revised: June 12, 2024

Accepted: June 16, 2024

Published: June 20, 2024



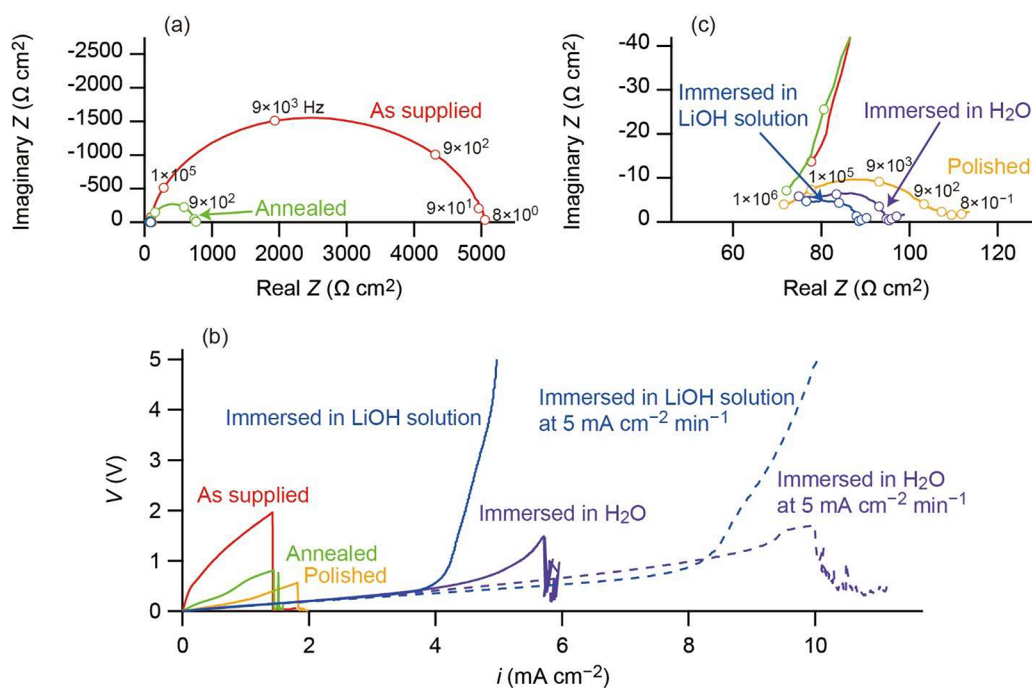


Figure 1. Electrochemical behaviors of Li/garnet/Li symmetric cells. (a) Nyquist plots before the i - V measurement and (b) i - V characteristics observed under the ramp-up current. Parts of the Nyquist plots in (a) are enlarged in (c), and some data points are labeled with the measured frequencies. The ramp-up current rate in (b) is $1.0 \text{ mA cm}^{-2} \text{ min}^{-1}$ unless otherwise indicated, and the cells are operated at $25 \text{ }^\circ\text{C}$.

semicircle corresponds to the sum of the charge transfer resistance at two Li/garnet interfaces, interfacial resistance can be estimated to be $2.5 \text{ k}\Omega \text{ cm}^2$. The ramp-up current applied to the cell causes an abrupt drop of the cell voltage to 0 V at a current density of 1.4 mA cm^{-2} due to the internal short-circuit, as shown in Figure 1b.

If the large interfacial resistance originates from the contamination layer, a simple way to reduce the resistance is removing the contamination layer by polishing.^{10,11} Indeed, polishing the pellet surface dramatically reduces the interfacial resistance to $20 \text{ }\Omega \text{ cm}^2$, as shown in Figure 1c; however, it hardly increases the critical current density: the critical current density is increased only to 1.8 mA cm^{-2} , as can be seen in Figures 1b. Another method reported to remove the contamination layer is heat treatment: it was reported that annealing at $250 \text{ }^\circ\text{C}$ reacts contaminated Li_2CO_3 with the proton-exchanged garnet to recover the garnet surface and structure and reduce the interfacial resistance.¹² However, annealing at $700 \text{ }^\circ\text{C}$ in this study does not improve the performance of the lithium metal electrode: interfacial resistance increases again to $650 \text{ }\Omega \text{ cm}^2$, and critical current density decreases back to 1.4 mA cm^{-2} , as shown in panels a and b of Figure 1, respectively.

Remarkable improvements are brought about by immersion in the LiOH solution, as demonstrated in Figure 1b,c. In this treatment, the pellet is immersed in a saturated aqueous solution of LiOH, which is prepared by dissolving an excess amount of LiOH·H₂O in deionized water and should be 5.3 M in concentration according to the saturation solubility. After immersion, the pellet is rinsed in a diluted LiOH solution (pH 14) and then the residual solution on the rinsed pellet is blown off by a N_2 stream. The pellet is not rinsed in pure water because it may cause proton exchange. It decreases the interfacial resistance to $10 \text{ }\Omega \text{ cm}^2$, which is lower than that reported for the interface treated with carbon.¹³ In addition,

the cell voltage does not exhibit an abrupt drop up to 5.0 mA cm^{-2} , and instead, it increases and reaches 5 V at this current density. The absence of a voltage drop indicates that internal short-circuit does not happen up to this current density, and the increase in the cell voltage may originate from the depletion of lithium metal in the counter electrode; however, the counter electrode has a sufficient amount of lithium metal for chronopotentiometry. The areal capacity to the end of the measurement is 0.21 mAh cm^{-2} , and the thickness of lithium metal stripped from the counter electrode estimated from the areal capacity is $1.0 \text{ }\mu\text{m}$, as listed in Table S1 in the Supporting Information, while the thickness of lithium metal formed on the pellet by thermal evaporation is $5 \text{ }\mu\text{m}$. Therefore, the increase in the cell voltage should be attributed to loss of contact between the garnet pellet and lithium metal; the large amount of stripped lithium forms many voids at the interface.

Increasing the ramp-up rate will enable us to determine the critical current density in the higher current region because it reduces the consumption of lithium metal in the counter electrode during the measurement. However, even when the current ramp-up rate is increased to $5 \text{ mA cm}^{-2} \text{ min}^{-1}$, internal short-circuit does not take place up to 10 mA cm^{-2} , at which the estimated thickness of lithium metal from the counter electrode approaches $1 \text{ }\mu\text{m}$ and the cell voltage reaches 5 V again, as shown in Table S1 and Figure 1b, respectively. These results strongly demonstrate that immersion in a LiOH solution is effective in increasing critical current density.

The differences in the electrode properties will originate from changes in the pellet surface that form interfaces with lithium metal electrodes, and the changes can be followed by grazing incidence X-ray diffraction (GIXRD) at an incident angle of 0.25° and secondary ion mass spectrometry (SIMS). The diffraction patterns are taken using Cu-K α radiation, and the depth profiles are recorded on a mass spectrometer using a primary ion beam of Cs^+ . Li_2CO_3 and LiOH, which are

possible contaminants, are detectable in the SIMS measurement as the signals of ^{12}C and ^1H , respectively. On the other hand, immersion in the aqueous solution of LiOH may induce Li^+/H^+ exchange. Therefore, the samples for the SIMS measurement are immersed in a heavy water solution of LiOH in order to distinguish ^1H in contaminant LiOH from ^2D introduced during the immersion.

Since the as-supplied pellet shows large interfacial resistance to the lithium metal electrode, a contamination layer that impedes charge transfer at the Li/garnet interface will be formed on the surface of the pellet. However, it is not observed even in the surface-sensitive GIXRD pattern displayed in Figure 2a, and all of the diffractions in the GIXRD pattern are

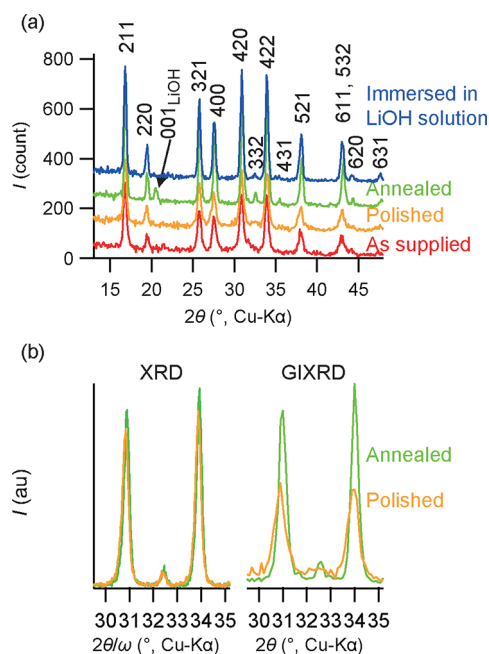


Figure 2. XRD patterns for the garnet pellets. (a) GIXRD patterns for the pellets before and after the treatments. Reflections in (a) are indexed on the basis of the cubic garnet structure. (b) Comparison of GIXRD and XRD patterns for the pellets after polishing and annealing.

attributable to the cubic garnet structure. On the other hand, the depth profile obtained by SIMS clearly reveals the contamination. Signal intensity for Zr and La decreases and that for C and H increases at the pellet surface, as shown in Figure 3, which suggests that the contaminants are LiOH and Li_2CO_3 , and they are present over a range of $2\ \mu\text{m}$ from the surface. Because the contaminants are generated by exposure to ambient air at room temperature, their crystallinity will be low, which is the reason for the absence of their diffractions in the GIXRD pattern.

Since the thickness of the contamination layer is $2\ \mu\text{m}$, it will be readily removed by polishing. In fact, it significantly reduces the resistance at the Li/garnet interface from $2.5\ \text{k}\Omega\ \text{cm}^{-2}$ to $20\ \Omega\ \text{cm}^{-2}$; however, it hardly increases the critical current density, which may be due to the polishing damage. Figure 2b compares the diffraction patterns for the pellets before and after annealing recorded by normal ω - 2θ X-ray diffraction (XRD) and GIXRD. The annealing increases the diffraction intensity observed in the XRD pattern to some extent, whereas the increase in the diffraction intensity is significant in the

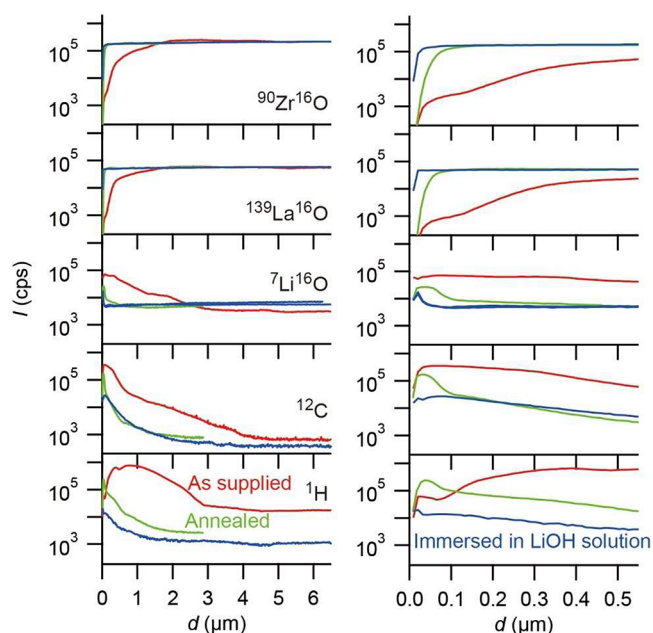


Figure 3. SIMS depth profiles of the pellets. Signal intensities are plotted against the depth from the pellet surface, d , in the left panel, and the profiles in $d = 0\text{--}0.55\ \mu\text{m}$ are enlarged on the right.

GIXRD pattern. Because GIXRD collects diffraction from the surface of the sample, the remarkable increase in the diffraction intensity observed in the GIXRD pattern indicates that crystallinity near the surface is low after polishing; that is, the surface of the garnet pellet forming the interface to the metal lithium electrode suffers polishing damage.

Annealing eliminates the polishing damage, which can be recognized as the increasing diffraction intensity, as shown in Figure 2b. However, it increases the interfacial resistance and decreases the critical current density, which is due to reformation of a contamination layer. Strong signals for C and H observed in the SIMS depth profiles at the pellet surface, where signals for Zr and La are weakened, suggest that LiOH and Li_2CO_3 exist as the contaminants in the surface region with $0.1\ \mu\text{m}$ in depth, and a diffraction at $2\theta = 20.5^\circ$ appearing in the GIXRD pattern is attributable to the 001 reflection from LiOH. That is, the annealing segregates the residual contaminants inside the pellet after the polishing to form a contamination layer on the surface again, which increases the interfacial resistance and decreases the critical current density.

Immersion in a LiOH solution successfully removes the contaminant layer without damaging the solid electrolyte. The depth profiles in Figure 3 indicate that contents of C and H at the surface decrease significantly by the immersion. Moreover, immersion does not decrease the diffraction intensity from the garnet, as shown in Figure 2a. It should be noted that the final treatment should be done in a LiOH solution. Immersion in water also removes LiOH and Li_2CO_3 from the surface to decrease the interfacial resistance to $10\ \Omega\ \text{cm}^2$, as demonstrated in Figure 1c. However, the immersion exchanges the lithium ions in the solid electrolyte with protons to deteriorate Li transfer kinetics in the Li/garnet interface.¹⁴ In fact, the critical current density after immersion in water is $5.7\ \text{mA}\ \text{cm}^{-2}$ under the ramp-up current rate of $1\ \text{mA}\ \text{cm}^{-2}\ \text{min}^{-1}$, as shown in Figure 1b. Under the higher ramp-up rate of $5\ \text{mA}\ \text{cm}^{-2}\ \text{min}^{-1}$, a voltage drop does not appear at the current

density of 5.7 mA cm^{-2} , which is because dendrites do not grow enough to bridge between the working and counter electrodes. Increasing the ramp-up current rate decreases the amount of deposited lithium metal when the ramp-up current reaches the same current density. Even so, internal short-circuit takes place at 10 mA cm^{-2} . Such proton exchange can be avoided in the LiOH solution.¹⁵

This surface treatment enabled us to assemble a solid-state battery with a garnet electrolyte. The cathode of this battery is a mixture of LiCoO_2 and the solid electrolyte applied on a sintered pellet of garnet and heated at $700 \text{ }^\circ\text{C}$, and the anode is a Li foil attached to the other side of the pellet. A 23 nm thick Ta layer and a 5.7 nm thick In layer are deposited as the interlayers on the cathode and anode sides, respectively. Details of the battery assembly will be reported elsewhere.¹⁶ Figure 4a shows charge–discharge curves of the battery at

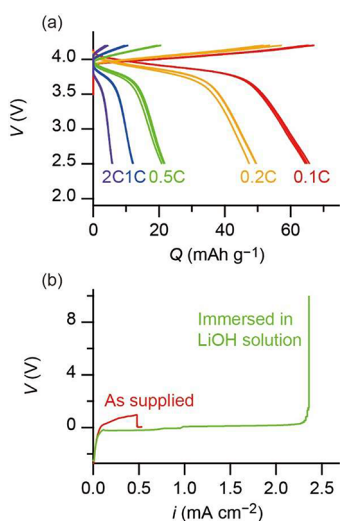


Figure 4. (a) Charge–discharge curves of a Li/garnet/ LiCoO_2 solid-state battery with various charge–discharge rates and (b) i – V characteristics observed for Li/garnet/Au cells. The horizontal axis in (a) indicates the specific capacity (Q) based on the weight of LiCoO_2 . The battery is cycled four times in each C-rate in constant-current charge–discharge mode, and typical charge–discharge curves are presented in the figure.

various charge–discharge rates under constant-current conditions. The charge–discharge rates increase from 0.1C to 2C, which correspond to the current densities from 7.7 to $150 \mu\text{A cm}^{-2}$, and the battery is cycled four times in each C-rate. The battery does not reach an internal short-circuit during the cycling.

The surface treatment is also effective in suppressing dendritic growth in Li-free batteries. The Li-free battery does not have lithium metal in its anode when assembled, and a lithium metal anode is formed on the anode current collector *in situ* during the first charging.¹⁷ The current collector is generally made of Cu, and thus, effects of the surface treatment on the dendritic growth at the Li-free anode can be evaluated in a Li/garnet/Cu asymmetric cell. However, the as-supplied sintered pellet shows interfacial resistance exceeding $50 \text{ k}\Omega \text{ cm}^2$ to the *in situ* plated Li anode on the Cu current collector. Therefore, a Au interlayer with 94 nm in thickness is formed on the garnet pellet to reduce the resistance¹⁸ and perform the chronopotentiometry. Figure 4b compares the chronopotentiograms for the Li/garnet/Au asymmetric cells with the as-

supplied pellet and immersed in the LiOH solution under a current ramp-up rate of $0.1 \text{ mA cm}^{-2} \text{ min}^{-1}$. The cell with the as-supplied pellet reaches an internal short-circuit at 0.48 mA cm^{-2} . This value is lower than that observed for the Li/garnet/Li cell in Figure 1b. The reason is that the internal short-circuit tends to take place at a higher current density under a higher current ramp-up rate, as discussed above, and vice versa. When the current ramp-up rate is set to $1 \text{ mA cm}^{-2} \text{ min}^{-1}$, the Li/garnet/Au cell reached an internal short-circuit at the higher current density of 1.5 mA cm^{-2} . On the other hand, internal short-circuit is not observed at least until 7 mA cm^{-2} for the cell assembled with the pellet after immersion in the LiOH solution.

This study demonstrates that immersion in an aqueous solution of LiOH is a simple and effective way to suppress internal short-circuit occurring in a solid-state battery with a lithium metal electrode and a garnet-type solid electrolyte by removing the contamination layer that forms on the surface of the solid electrolyte. Because many studies have revealed that lithium dendrites grow and penetrate through garnet pellets along the grain boundaries,^{6,19} influence of the LiOH solution on grain boundaries should be noted. It is not possible to consider that the immersion in this study affects the propagation of lithium metal through the grain boundaries because the sintered pellets used in this study are dense. The relative density is around 97%, and there are few voids in the pellets, as shown in the cross-sectional secondary electron micrograph in Figure S1 in the Supporting Information. Therefore, the LiOH solution will not infiltrate into the pellet during the immersion to affect the grain boundaries.

In addition, this study suggests that only reduction of the resistance at the Li/garnet interface is not enough to avoid the short-circuit, as indicated by the critical current densities observed for the surface-polished solid electrolyte and that immersed in water. Although the reason for this has not been fully understood, it may be because these treatments induce inhomogeneity in the current density. The protonation caused by immersion in water is reported to lower the transfer kinetics at the Li/garnet interface, as mentioned above. In addition, since lowering crystallinity decreases the ionic conductivity,²⁰ polishing damage will also block the ionic diffusion. These defects scattered at the interface make current density inhomogeneous, and the local current density can exceed the critical value for the internal short-circuit.

■ ASSOCIATED CONTENT

Supporting Information

The Supporting Information is available free of charge at <https://pubs.acs.org/doi/10.1021/acsaem.4c00805>.

Cross-sectional scanning electron micrograph of a sintered garnet pellet and estimated thickness of plated Li at the internal short-circuit or at the end of the measurements (PDF)

■ AUTHOR INFORMATION

Corresponding Author

Kazunori Takada – Research Center for Energy and Environmental Science, National Institute for Materials Science, Tsukuba, Ibaraki 305-0044, Japan; orcid.org/0000-0001-7568-1806; Phone: +81 29 8604317; Email: takada.kazunori@nims.go.jp

Authors

Tsuyoshi Ohnishi – Research Center for Energy and Environmental Science, National Institute for Materials Science, Tsukuba, Ibaraki 305-0044, Japan; orcid.org/0000-0002-2333-7752

Isao Sakaguchi – Research Center for Electronic and Optical Materials, National Institute for Materials Science, Tsukuba, Ibaraki 305-0044, Japan; orcid.org/0000-0003-4382-2509

Complete contact information is available at:
<https://pubs.acs.org/10.1021/acsaem.4c00805>

Notes

The authors declare no competing financial interest.

ACKNOWLEDGMENTS

The authors would like to thank Ms. Mai Uchida and Ms. Naomi Tsurumi for their assistance in scanning electron microscopy. This work was partly supported by the Advanced Low Carbon Technology Research and Development Program, Specially Promoted Research for Innovative Next Generation Batteries (ALCA-SPRING) of the Japan Science and Technology Agency (JST), Japan (grant number JPMJAL1301); GteX Program of JST, Japan (grant number JPMJGX23S2); Materials Processing Science project (“Materealize”) of Ministry of Education, Culture, Sports, Science and Technology (MEXT), Japan (grant number JPMXP0219207397); and the Program on Open Innovation Platforms for Industry-academia Co-creation of JST (grant number JPMJPF2016).

REFERENCES

- (1) Aono, H.; Sugimoto, E.; Sadaoka, Y.; Imanaka, N.; Adachi, G. Ionic Conductivity of Solid Electrolytes Based on Lithium Titanium Phosphate. *J. Electrochem. Soc.* **1990**, *137*, 1023–1027.
- (2) Inaguma, Y.; Liqun, C.; Itoh, M.; Nakamura, T.; Uchida, T.; Ikuta, H.; Wakihara, M. High Ionic Conductivity in Lithium Lanthanum Titanate. *Solid State Commun.* **1993**, *86*, 689–693.
- (3) Li, Y.; Han, J.-T.; Wang, C.-A.; Xie, H.; Goodenough, J. B. Optimizing Li⁺ Conductivity in a Garnet Framework. *J. Mater. Chem.* **2012**, *22*, 15357–15361.
- (4) Thangadurai, V.; Weppner, W. Li₆Al₂Ta₂O₁₂ (A = Sr, Ba): Novel Garnet-Like Oxides for Fast Lithium Ion Conduction. *Adv. Funct. Mater.* **2005**, *15*, 107–112.
- (5) Zhu, Y.; Connell, J. G.; Tepavcevic, S.; Zapol, P.; Garcia-Mendez, R.; Taylor, N. J.; Sakamoto, J.; Ingram, B. J.; Curtiss, L. A.; Freeland, J. W.; Fong, D. D.; Markovic, N. M. Dopant-Dependent Stability of Garnet Solid Electrolyte Interfaces with Lithium Metal. *Adv. Energy Mater.* **2019**, *9*, 1803440.
- (6) Ren, Y.; Shen, Y.; Lin, Y.; Nan, C.-W. Direct Observation of Lithium Dendrites Inside Garnet-Type Lithium-Ion Solid Electrolyte. *Electrochem. Commun.* **2015**, *57*, 27–30.
- (7) Cheng, E. J.; Sharafi, A.; Sakamoto, J. Intergranular Li Metal Propagation Through Polycrystalline Li_{6.25}Al_{0.25}La₃Zr₂O₁₂ Ceramic Electrolyte. *Electrochim. Acta* **2017**, *223*, 85–91.
- (8) Cheng, L.; Crumlin, E. J.; Chen, W.; Qiao, R.; Hou, H.; FranzLux, S.; Zorba, V.; Russo, R.; Kostecki, R.; Liu, Z.; Persson, K.; Yang, W.; Cabana, J.; Richardson, T.; Chen, G.; Doeff, M. The origin of high electrolyte-electrode interfacial resistances in lithium cells containing garnet type solid electrolytes. *Phys. Chem. Chem. Phys.* **2014**, *16*, 18294–18300.
- (9) Sharafi, A.; Yu, S.; Naguib, M.; Lee, M.; Ma, C.; Meyer, H. M.; Nanda, J.; Chi, M.; Siegel, D. J.; Sakamoto, J. Impact of Air Exposure and Surface Chemistry on Li-Li₇La₃Zr₂O₁₂ Interfacial Resistance. *J. Mater. Chem. A* **2017**, *5*, 13475–13487.
- (10) Ma, X.; Xu, Y. Effects of Polishing Treatments on the Interface Between Garnet Solid Electrolyte and Lithium Metal. *Electrochim. Acta* **2023**, *441*, 141789.
- (11) Sharafi, A.; Kazyak, E.; Davis, A. L.; Yu, S.; Thompson, T.; Siegel, D. J.; Dasgupta, N. P.; Sakamoto, J. Surface Chemistry Mechanism of Ultra-Low Interfacial Resistance in the Solid-State Electrolyte Li₇La₃Zr₂O₁₂. *Chem. Mater.* **2017**, *29*, 7961–7968.
- (12) Cheng, L.; Liu, M.; Mehta, A.; Xin, H.; Lin, F.; Persson, K.; Chen, G.; Crumlin, E. J.; Doeff, M. Garnet Electrolyte Surface Degradation and Recovery. *ACS Appl. Energy Mater.* **2018**, *1*, 7244–7752.
- (13) Li, Y.; Chen, X.; Dolocan, A.; Cui, Z.; Xin, S.; Xue, L.; Xu, H.; Park, K.; Goodenough, J. B. Garnet Electrolyte with an Ultralow Interfacial Resistance for Li-Metal Batteries. *J. Am. Chem. Soc.* **2018**, *140*, 6448–6455.
- (14) Brugge, R. H.; Hekselman, A. K. O.; Cavallaro, A.; Pesci, F. M.; Chater, R. J.; Kilner, J. A.; Agudero, A. Garnet Electrolytes for Solid State Batteries: Visualization of Moisture-Induced Chemical Degradation and Revealing Its Impact on the Li-Ion Dynamics. *Chem. Mater.* **2018**, *30*, 3704–3713.
- (15) Ma, C.; Rangasamy, E.; Liang, C.; Sakamoto, J.; More, K. L.; Chi, M. Excellent Stability of a Lithium-Ion-Conducting Solid Electrolyte upon Reversible Li⁺/H⁺ Exchange in Aqueous Solutions. *Angew. Chem., Int. Ed.* **2015**, *54*, 129–133.
- (16) Mitsuishi, K.; Ohnishi, T.; Niitsu, K.; Masuda, T.; Takada, K. Lowering the Sintering Temperature of LiCoO₂ Using LiOH Aqueous Solution. *Solid State Ionics* **2024**, submitted for publication.
- (17) Neudecker, B. J.; Dudney, N. J.; Bates, J. B. Lithium-Free^{*} Thin-Film Battery with *In Situ* Plated Li anode. *J. Electrochem. Soc.* **2000**, *147*, 517–523.
- (18) Alexander, G. V.; Patra, S.; Sobhan Raj, S. V.; Sugumar, M. K.; Ud Din, M. M.; Murugan, R. Electrode-Electrolyte Interfacial Engineering for Realizing Room Temperature Lithium Metal Battery Based on Garnet Structured Solid Fast Li⁺ Conductors. *J. Power Sources* **2018**, *396*, 764–773.
- (19) Ren, Y.; Shen, Y.; Lin, Y.; Nan, C.-W. Direct Observation of Lithium Dendrites Inside Garnet-Type Lithium-Ion Solid Electrolyte. *Electrochem. Commun.* **2015**, *57*, 27–30.
- (20) Hanft, D.; Exner, J.; Moos, R. Thick-Films of Garnet-Type Lithium Ion Conductor Prepared by the Aerosol Deposition Method: The Role of Morphology and Annealing Treatment on the Ionic Conductivity. *J. Power Sources* **2017**, *361*, 61–69.